A combined theoretical-experimental study on the acidity of WO(x)-ZrO(2) systems

ARTICLE *in* PHYSICAL CHEMISTRY CHEMICAL PHYSICS · AUGUST 2008

Impact Factor: 4.49 · DOI: 10.1039/b802934b · Source: PubMed

3 AUTHORS, INCLUDING:

Annia Galano
Metropolitan Autonomous University
152 PUBLICATIONS **3,287** CITATIONS
SEE PROFILE

E. Torres-García
Instituto Mexicano del Petroleo
43 PUBLICATIONS **735** CITATIONS
SEE PROFILE

A combined theoretical–experimental study on the acidity of WO_x-ZrO_2 systems

Annia Galano,[a] Geonel Rodriguez-Gattorno[b] and Enelio Torres-García*[c]

Received 20th February 2008, Accepted 21st April 2008
First published as an Advance Article on the web 5th June 2008
DOI: 10.1039/b802934b

This work provides a chemical approach to the relationship between structure and electronic behavior of the active surface of the WO_x-ZrO_2 system as a function of W loads. This study shows that the electronic hardness (η), the Lewis and Brønsted acidity are functions of the local coordination and of the polymerization degree of the WO_x domain. From theoretical calculations the observed behavior in the WO_x-ZrO_2 system is explained: the Brønsted acidity increases while the Lewis acidity decreases as the W centers go from tetrahedral to octahedral coordination and as the condensation degree of the WO_x domain increases. Our results also indicate that not all the Brønsted sites in the WO_x domains are equally acid, and that as the W load increases the most acid sites decrease in number due to the condensation process. This finding also means a decrease on the average acidity per H site. Additionally, our results suggest that for surface densities in the 4–7 W nm^{-2} range, mainly dimeric-tungstate species are present. A maximum in Brønsted acidity was observed for a W surface density about 7 W nm^{-2}.

Introduction

Since the first report on the generation of strong acid sites on supported tungsten oxide on zirconia by Hino and Arata,[1,2] the WO_x-ZrO_2 system has received much attention. This has been caused by its good combination of activity and selectivity in reactions such as hydrocarbon isomerization, ring opening, dehydration, *etc*. This pleasing behavior has been explained as a consequence of balanced surface acid properties, density of acid sites, and high thermal stability.[3–8]

It is generally accepted that the WO_x-ZrO_2 system possesses both Lewis and Brønsted acidity, although their detailed structures are still actively debated. Afanasiev *et al*.[9] proposed a structural model for the WO_x-ZrO_2 system in which hydrated zirconia oxide was coordinated to several tungsten oxo-anions, and the OH groups were solely attached to the Zr atom, generating the Brønsted acid sites. Other authors[4,10,11] have proposed that the generation of Brønsted sites was attributed to H_2 dissociation on Lewis sites in the form of W^{6+} centers and that the $H^{+\delta}$ is stabilized by WO_x clusters through electron transfer and charge delocalization. More recently, Gregorio and Keller[12] have suggested that a condensation phenomenon of superficial tungstate monomeric species takes place, leading to the formation of polymeric species in which a combination of Lewis and Brønsted acidic sites is present. The trends in acid–base behavior of solids are crucial parameters for the explanation of catalyzed reactions. Regardless of the extensive studies on the WO_x-ZrO_2 system, little attention has been focused on establishing and justification, from a theoretical point of view, of the relationship between catalytic efficiency and surface acid–base properties. The WO_x-ZrO_2 system requires an exact control of surface acid properties, especially for those reactions where the catalytic activity is justified by Brønsted acidity.

In the present work, a series of catalysts with different tungsten (W) loadings were prepared by the impregnation method using zirconia as the support.[13] The results obtained from different techniques in previous works were used to propose a chemical approach to the relationship between structure and electronic behavior of the active surface as a function of W loads.[13,14] Theoretical calculations were performed on several models in order to explain acid–base trends in WO_x-ZrO_2 systems. To our knowledge, this is the first systematic study that reaches an adequate balance between experimental results and theoretical predictions.

Experimental

WO_x-ZrO_2 was prepared by impregnation following a procedure previously reported.[13] High-surface-area $ZrO_{2-x}(OH)_{2x}$ (320 m^2 g^{-1}) was prepared by hydrolysis of 0.5 M zirconyl chloride solution ($ZrOCl_2{\cdot}8H_2O$, Aldrich, >98 wt%) at a pH of 10 using NH_4OH. The resulting solid was filtrated and washed repeatedly by redispersion with a NH_4OH solution (pH = 10) until the elimination of chloride ions and then dried at 383 K for 24 h. $ZrO_{2-x}(OH)_{2x}$ was impregnated with an ammonium metatungstate solution ($(NH_4)_6H_2W_{12}O_{40}$, Strem Chemicals, 99.9%) maintaining the pH at 10. Finally, WO_x-ZrO_2 samples were treated in flowing dry air for 3 h at 1073 K. The stabilized surface area of WO_x-ZrO_2 in calcined samples was about 40–60 m^2 g^{-1}. WO_x surface densities were varied by

[a] *Departamento de Química, Universidad Autónoma Metropolitana-Iztapalapa, San Rafael Atlixco 186, Col. Vicentina, Iztapalapa, México, D.F., México C.P. 09340*
[b] *Centro de Investigaciones en Ciencias Aplicadas y Tecnologías Avanzadas del IPN, Legaria 694, Col. Irrigación, Del. Miguel Hidalgo, México D.F., México CP 11500*
[c] *Instituto Mexicano del Petróleo, Eje Central Norte, Lázaro Cárdenas 152, San Bartolo Atepehuacan, 07730 México D.F., México. E-mail: etorresg@imp.mx, eneliot@yahoo.es; Fax: +52-55-91758429; Tel: +52-55-91758430*

changing the tungsten (W) concentration in order to obtain samples with WO_x surface densities between 2–16 W nm^{-2}.

The optical characterization was realized by diffuse reflectance with a Varian (Cary 5E) spectrophotometer and Kubelka-Munk function (FKm) was used to convert reflectance measurements (R_{sample}) into equivalent absorption profiles, see details in ref. 13. Brønsted and Lewis acidity of samples with different tungsten loading was monitored by pyridine adsorption FT-IR spectroscopy (NICOLET Model 60SXB, 4 cm^{-1} resolution and average over 500 scans). The calcined powder samples in a sample holder were placed in a specially designed cell. The samples were then heated *in situ* from room temperature to 673 K at a heating rate of 5 K min^{-1} in a flowing stream (40 mL min^{-1}) of N_2. The samples were kept at 673 K for 3 h and then cooled to room temperature. Finally, pyridine vapor (20 μL) was introduced under N_2 flow at room temperature, evacuated and the IR spectra were recorded at 373 K.

Computational details

The theoretical calculations have been carried out with Gaussian 98[15] package of programs within the density functional theory (DFT) formalism. Geometry optimizations have been performed using the generalized gradient approximation (GGA), without any symmetry constraint. The Perdew and Wang's 1991[16] functional (PW91) was used for exchange and correlation potentials. We have used the Dunning/Huzinaga valence double-zeta D95V[17] basis set for O, C, N and H atoms and the Stuttgart/Dresden[18] relativistic effective core potential (ECP) for W and Zr. Frequency calculations were carried out for all the studied systems at the same level of theory. Thermodynamic corrections at 298.15 K were included in the calculation of the relative energies.

The global hardness η, defined by Parr and Pearson[19] as the second derivative of the electronic energy of the system with respect to the number of electrons at a constant external potential:

$$\eta = \frac{1}{2}\left(\frac{\partial^2 E}{\partial N^2}\right)_{\nu(r)} \quad (1)$$

has been calculated in a finite-difference approximation, with the assumption that the energy varies quadratically with the number of electrons, as:

$$\eta = \frac{I - A}{2} \quad (2)$$

where I and A are the ionization potential and the electron affinity, respectively; and according to Koopmans' theorem:

$$\eta = \frac{I - A}{2} = \frac{-(E_{HOMO} - E_{LUMO})}{2} \equiv \frac{E_{LUMO} - E_{HOMO}}{2} \equiv \frac{E_{gap}}{2} \quad (3)$$

where E_{LUMO} and E_{HOMO} are Kohn–Sham one-electron eigenvalues associated with the lowest unoccupied molecular orbital (LUMO) and the highest occupied molecular orbital (HOMO), respectively, and they are obtained from DFT calculations of the neutral species. Additionally and to compare with the experimental values, the E_{gap} was also estimated from the UV/Vis spectra computed using time dependent (TD) DFT calculations as the excitation energy corresponding to λ_{max}. TD-DFT[20] can be viewed as an exact reformulation of the time-dependent quantum mechanics, and it has become one of the most popular methods for the calculations of electronic spectra and excited states of medium-sized and large molecules.[21] Even though TD-DFT introduces errors by using approximate exchange–correlation functionals it has being improved for long-range charge-transfer excited states.[22]

The condensed Fukui functions (FF) have been obtained at the optimized geometries with DMOL3 code[23,24] through the Material Studio user interface, using the PW91 functional and double numerical with polarization functions (DNP) basis set + DFT Semi-core Pseudopots (DSPP). Since we are interested in the acidity of the H sites, we have focused our attention on the nucleophilic FF, f_k^+, which measures changes in the electron density when the molecule gains electrons. These functions are computed using the finite difference approximation and the self-consistent charge densities for the neutral molecule and the anion, as:

$$f_k^+ = q_k^{anion} - q_k \quad (4)$$

where q_k represent atomic-centered charges, obtained from the Hirshfeld partitioning scheme.[25]

Results and discussion

We recently reported that the WO_x-ZrO_2 system with a load of $\sim$7 W nm^{-2} is composed of ZrO_2 nanometric particles ($\leq$20 nm), surrounded by a shell-like WO_x layer.[13,14] Our results and previous reports[5,26,27,33] are consistent with the fact that at low surface WO_x density ($\leq$4 W nm^{-2}), isolate monomeric species are present. At higher surface density (within 4–7 W nm^{-2}), both monomeric and polymeric surface WO_x species coexist, the proportion of the latter increases with the WO_x surface coverage. For values above 9 W nm^{-2}, crystalline WO_3 clusters have been observed.[13,28,29] Additionally, from analysis of the band gap energy (E_{gap}) measurements it was demonstrated that the surface transformation of monomeric to polymeric species, implicates a change in domain size affecting the surface electronic properties of the samples and that the hardness drastic decay when the W content is increased. Thus, in the present case, the electronic hardness is a function of the local structure, polymerization degree and domain size as a result of the increase in electron localization due to electron confinement.[13]

In the present work we investigate the surface acid–base properties of the WO_x-ZrO_2 system. The Brønsted and Lewis acidity of samples with different W loads was measured by pyridine adsorption *in situ* using FT-IR spectroscopy (see Fig. 1). FT-IR spectra of these samples present bands at 1444, 1488 and 1539 cm^{-1}, as well as a group of bands in the region 1580–1620 cm^{-1}. The bands at 1444 cm^{-1} and the group at 1580–1620 cm^{-1} are characteristic of pyridine coordinated to Lewis acid sites. The intensity of the 1444 cm^{-1} band is proportional to the total number of Lewis sites, whereas the positions of the bands in the group at 1580–1620 cm^{-1} are sensitive to the strength of these sites.[30]

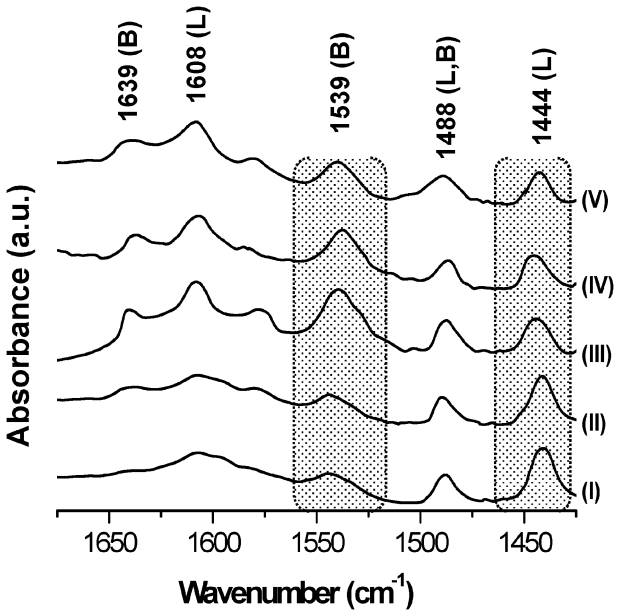

Fig. 1 The infrared spectra of pyridine adsorption on WO_x-ZrO_2 as a function of surface density (W nm^{-2}) samples. (I) 1.93 W nm^{-2}; (II) 4.01 W nm^{-2}; (III) 7.02 W nm^{-2}; (IV) 9.3 W nm^{-2} and (V) 12.2 W nm^{-2}.

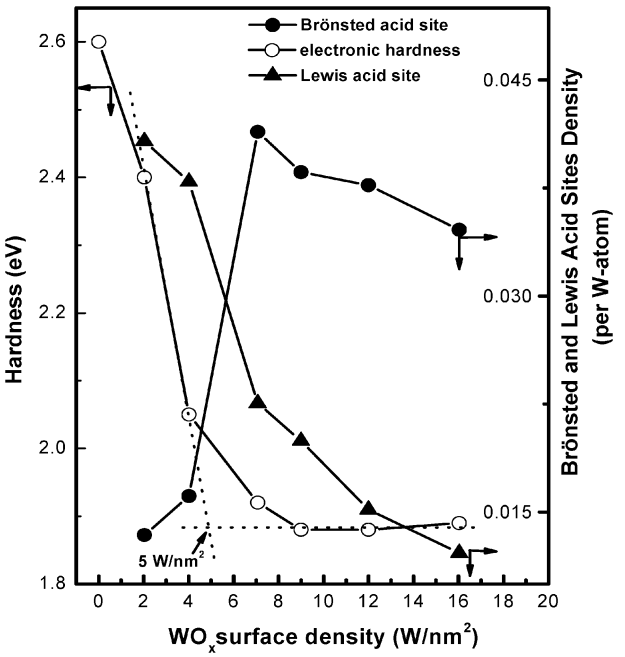

Fig. 2 Surface acid site density from FT-IR integrated peaks areas for pyridine adsorption as a function of W loading at 373 K. (●) *ca.* 1539 cm^{-1} (Brønsted sites); (▲) *ca.* 1444 cm^{-1} (Lewis sites) and electronic hardness (○) calculated from band gap energy (E_g) as a function of WO_x surface density (W nm^{-2}) on the ZrO_2 suport.

All these bands can be discerned in the spectra of the WO_x-ZrO_2 samples and the relative intensity and resolution of the bands at 1539 and 1608 cm^{-1} clearly increase with increasing W content, indicating that both Brønsted and Lewis sites are present at the surface of the WO_x-ZrO_2 system. From the FT-IR spectra, it is clear that the group bands at 1580–1620 cm^{-1} are composed of at least four distinct bands. However, we observe that the centre band at 1608 cm^{-1} gradually narrows down, and its intensity and resolution increase as a function of W loads, particularly for W concentrations higher than 7 W nm^{-2}. This behavior may be assigned to the formation of Lewis sites on WO_x species. The decreasing in the intensity of broad bands about 1580–1600 cm^{-1} suggests that the number of exposed Lewis sites on the support surface decreases as the WO_x surface coverage increases.

It is interesting to note that the band at 1539 cm^{-1}, which is characteristic of protonated pyridine, clearly grows with increasing W content. By contrast, the relative intensity of the band at 1444 cm^{-1} decreases with increasing W loading.

Fig. 2 summarizes the results of the density of Brønsted and Lewis acid sites determined by integration of the bands with absorption maxima at 1539 and 1444 cm^{-1}, respectively,[31] of the FT-IR spectrum of pyridine absorbed on different materials. Acid site densities were calculated using the integrated molar extinction coefficients published by Emeis[32] (1.67 and 2.22 cm μmol^{-1} for Brønsted and Lewis sites, respectively) and the areas of the peaks, normalized with respect to surface area.

The pyridine adsorption results show that the surface density of Brønsted acid site (per W-atom) increases exponentially with W loading between 4–7 W nm^{-2}. This zone is identified as the point where the polymeric species become the most abundant ones. On the other hand, the density of Lewis sites (per W-atom) decreases in a markedly non-linear fashion in the same zone up to reaching 7 W nm^{-2}, from this point on the decreasing becomes approximately linear (Fig. 2).

By contrast, the surface density of Brønsted acid sites decreases slightly for W concentrations higher than 7 W nm^{-2}. This decreasing would be motivated by the increase in the polymerization degree and/or in the numbers of W–O–W bonds, which leads to an overall lowering in the specific surface acidity, in agreement with the results reported by Iglesia *et al.*[4] and Wachs *et al.*[33]

Interestingly, the variation on Brønsted acidity reaches its maximun when hardness tends to its minimum (bulk WO_3). It is important to mention that the band gap (or hardness) is a global parameter giving the same information about the nature of the species present in this system,[13,26] however it does not have a direct relationship with the local reactivity.

In order to gain better understanding of their properties and of the relationship between local surface structure, acidity and electronic behavior of WO_x-ZrO_2 systems (as a function of W loads), several theoretical quantum calculations were accomplished.

Theoretical considerations

From a computational point of view, in order to achieve an optimum compromise between the computational cost and the quality of the results, the size of the model must be rather small, but at the same time large enough to reproduce the physical relevant features of the real systems. Different clusters structures have been used to mimic the studied compounds. Sun *et al.*[34] have used $(WO_3)_{1-4}$ clusters and show that even a dimer of tungsten oxide $(WO_3)_2$ possesses bulk-like features.

These authors found that the most stable structures of $(WO_3)_3$ and $(WO_3)_4$ are cyclic with each W bonded to four O, and with the W atoms connected *via* oxygen atoms forming regular structures with W–O–W sides. On the other hand, Broclawik *et al.*[35] have used WO_6 corner-sharing octahedral structural units, with the terminal O atoms saturated by H atoms which, according to these authors, closely resembles the building blocks encountered in many WO_3-related structures. In both works, four-W-centers clusters seem to be adequate for reproducing the physical behavior of the actual solid. Zirconia has also been successfully modeled using small clusters.[36,37] For the interphase WO_x-ZrO_2 Xu *et al.*[38] have used a Zr-four-center model, similar to that used in the present work. These authors have studied the nature of the Brønsted acid sites formed on this material with models involving protonated O atoms, *i.e.* comparing two different kinds of Brønsted sites: Zr–O–H and W–O(H)–Zr, to conclude that the latter arrangement show a higher acid character.

In the present work, we have tested different structures to model WO_x-ZrO_2 materials (Fig. 3). In all cases the bridging O atoms are considered as non-protonated since there is no experimental evidence indicating otherwise. In addition, and as it is going to be discussed later, there is no need to include O atoms with three chemical bonds to explain the Brønsted acidity of WO_x-ZrO_2 materials. The zirconia support has been modeled as a four Zr atoms fragment, all of them in tetrahedral configuration. This model actually mimics the most common surfaces found in zirconia {110}. Our model also reproduces the zirconia Zr–Zr experimental distance of 3.6 Å (JCPDS-#50-1089), in our model this distance was found to be equal to 3.9 Å. The computed Zr–O distance is 2.0 Å while the experimental values are 2.1 (JCPDS-#50-1089). For WO_x two kinds of structures have been considered corresponding to monomeric (I) and dimeric (II) species, in order to mimic different loads of WO_x on the zirconia surface. Structures II are assumed to be formed through a condensation process, *i.e.* IIb is formed by condensation of two Ib fragments, IIc from Ic, *etc*. In all cases the WO_x domains contain W(VI), with coordination numbers from 4 to 6, and structures from tetrahedral to octahedral. For all models the WO_x species are anchored on the zirconia surface through Zr–O–W bonds, and unidentate or bidentate structures have been considered. It has been experimentally estimated that the distances Zr–Zr, Zr–W and W–W in the WO_x-ZrO_2 systems are about 3.6–3.7 Å.[14] In our models the corresponding values are 3.7, 3.7 and 3.8 Å. The general agreement between the calculated and experimental geometrical parameters supports the validity of the models used in our calculations.

The calculated global hardness (η) of such systems is reported in Table 1. These magnitudes were calculated by the two different approaches described above. The agreement between the calculated values and those experimentally obtained for the zirconia model is very good. According to the experimental results reported in this work and in a previous publication[10,13] the η values of the WO_x-ZrO_2 materials are expected to range from 1.5 to 2.5 eV, depending on the W/Zr ratio. The values calculated in this work range from 1.5 to 2.03 eV for all the tested models. The calculations also reproduce the η tendency to decrease as the W surface density increases. Since numerous clusters were modeled, with

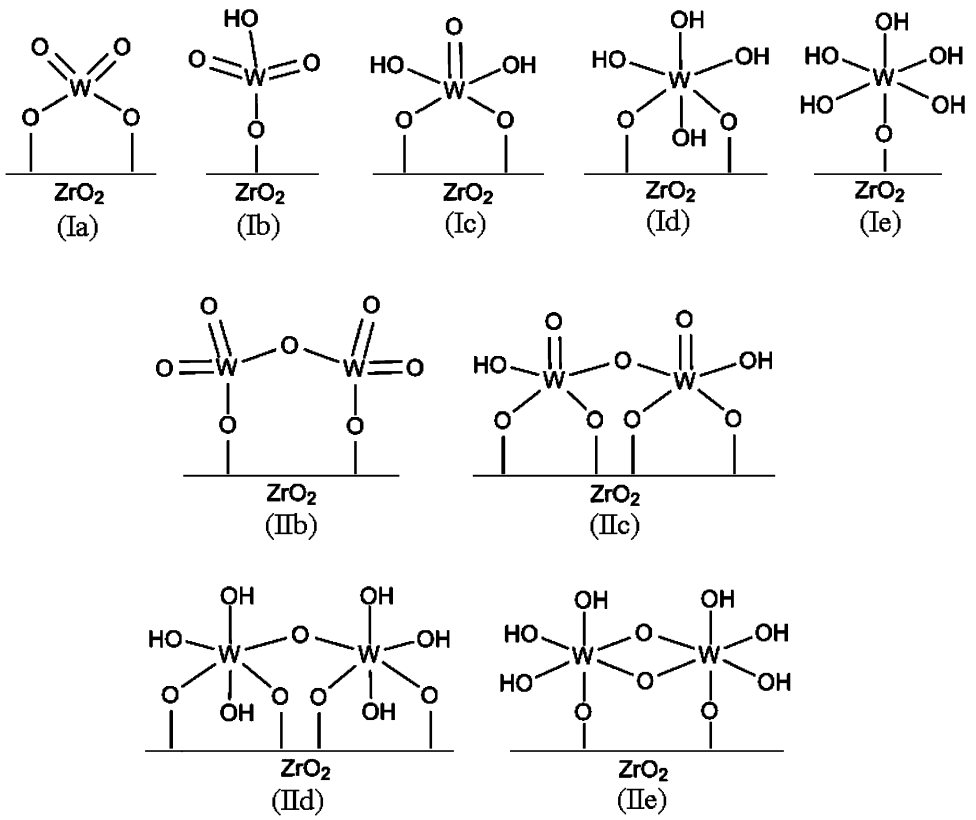

Fig. 3 Cluster models for monomeric and dimeric species anchored on the zirconia surface.

Table 1 Global hardness for the different tested models: from the frontier orbitals obtained by DFT calculation of the neutral species, and from the UV/Vis spectra obtained using TD-DFT

	η^{DFT}/eV	$\eta^{TD\text{-}DFT}$/eV
ZrO_2	2.59	2.60
Ia	1.92	2.03
Ib	1.86	1.89
Ic	1.61	1.71
Id	1.57	1.63
Ie	1.68	1.81
IIb	1.82	1.88
IIc	1.60	1.66
IId	1.38	1.54
IIe	1.49	1.54

different size and composition, the general agreement between experimental and calculated values validates the structures chosen for the theoretical calculations.

The Brønsted and Lewis acid strengths have been analyzed in terms of the energy release associated with the formation of pyridine adsorption products. The characteristic structures of such products are shown in Fig. 4, using model Ib as illustration. The relevant geometrical parameters involved in the formation of such adducts are reported in Table 2, together with the reaction enthalpies and Gibbs free energies. For WO_x-ZrO_2 systems the energy values correspond to pyridine adsorptions involving the most external hydroxyl groups in the WO_x domain. As the values in this table show, the presence of WO_x on the zirconia surface significantly increases the Brønsted acidity of the material. The energy release is larger and the r_1 (r_2) distances are shorter (larger) for any of the pyridine adsorption products on mixed surfaces, compared to that formed on pure zirconia. These geometrical parameters are enough to compare pure and WO_x loaded zirconia, however for comparisons among different mixed models the energetic criteria are more reliable and we will focus on them from now on. Analyzing the series I, from *a* to *e* in terms of the energy release involved in the pyridine adsorption, the Lewis acidity systematically decreases until the W atom is hexacoordinated and can not act as a Lewis acid. In the same direction within this series the acidity of Brønsted sites shows tendency to increase, with the exception of structure Ib. It should be noted that the values in Table 2 are calculated per H site, while the observed acidity depends not only on the intrinsic acidity of each site but also on the number of

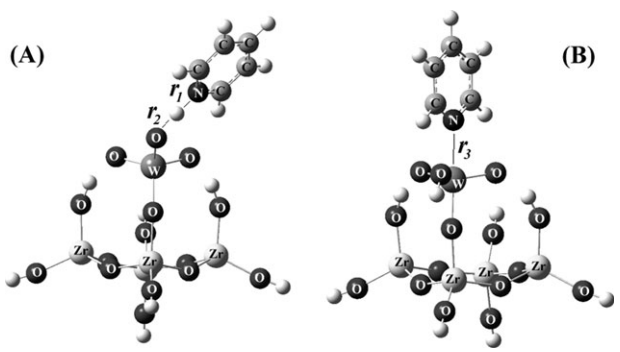

Fig. 4 Optimized geometries of characteristic adsorption products of pyridine on cluster Ib, involving Brønsted (A) and Lewis (B) sites.

Table 2 Enthalpies (ΔH) and Gibbs free energies (ΔG) of reaction for the adsorption process of pyridine on the modeled clusters, at 298 K; and selected geometrical parameters of the adsorbed products

	ΔH/kJ mol^{-1}	ΔG/kJ mol^{-1}	r_1/Å	r_2/Å	r_3/Å
Brønsted					
ZrO_2	−49	−18	1.576	1.037	
Ib	−108	−60	1.197	1.285	
Ic	−69	−22	1.140	1.369	
Id	−93	−43	1.218	1.256	
Ie	−144	−76	1.156	1.349	
IIc	−87	−43	1.308	1.175	
IId	−103	−53	1.163	1.329	
IIe	−86	−41	1.130	1.400	
Lewis					
Ia	−94	−46			2.311
Ib	−87	−34			2.307
Ic	−69	−23			2.407
IIb	−114	−62			2.297
IIc	−114	−61			2.292

Brønsted sites. Therefore, since the number of Brønsted sites (n_B) per W-atom increases in the series: n_B(Ia) = 0, n_B(Ib) = 1, n_B(Ic) = 2, n_B(Id) = 4, n_B(Ie) = 6, and the energy release associated to pyridine addition to cluster Ib is substantially less than twice that involving cluster Ic, the Brønsted acidity order in this series would be Ib < Ic < Id < Ie. Therefore, a generalization can be made: as the W center goes from tetrahedral to octahedral configuration the Brønsted acidity increases and the Lewis acidity decreases.

From all the used models there are only three of them that present both Brønsted and Lewis sites: Ib, Ic and IIc. Based on pyridine adsorption (Table 2) the acidity of structure Ib per Brønsted site is higher than its Lewis acidity. This is a straightforward comparison since there is one Brønsted site and one Lewis site in the modeled cluster. There is also the same number of Brønsted and Lewis sites in structure IIc, two in this case, and the Lewis acidity is higher than its Brønsted acidity. There are two main structural differences between structures Ib and IIc. The first one is that structure Ib is monomeric while IIc is dimeric, and the second one is that structure Ib is unidentate while IIc is bidentate. However, these results can not be used to draw conclusions related to the acid evolution of WO_x-ZrO_2 as the polymeric degree increases since the structures that are expected to be the most abundant ones in those systems as the polymeric degree increases are not IIc, but IId and IIe. The Ic structure has different numbers of Brønsted and Lewis sites: two and one, respectively. Accordingly, even though the corresponding values in Table 2 are very similar, it is expected that this structure has higher Brønsted acidity since the probability for pyridine to encounter a Brønsted site is twice that of encountering a Lewis site.

Comparing the corresponding structures in series I and II, it is clear that the number of Brønsted sites per W-atom decreases due to the condensation process, provided that the comparison is between species with the same W coordination number. Comparing structures Ie and IIe, in the dimeric specie not only the number of Brønsted sites decreases, but also does the site acidity. Going from Ic to IIc, and from Id to IId, the energy release per site increases, but not enough to overcome the reduction in the number of Brønsted sites. Accordingly, and assuming that the strength of the interaction would be

roughly the same for each site, the observed Brønsted acidity is predicted to decrease from monomer to dimer, and it seems reasonable to expect the same tendency from dimer to trimer, and so on. However, it should be noted that as the W load increases not only the polymeric/monomeric ratio rises but also does the octahedric-W/tetrahedric-W ratio.[13] Accordingly, the relevant comparisons are between monomeric structure Ib and dimers IId or IIe. Such comparisons show that the number of Brønsted sites is larger in dimers than in 2 monomeric units. Accordingly, the actual decrease in Brønsted acidity is expected to occur when the WO_x domains are mainly formed by WO_x domains with larger polymeric degrees. In addition, the Brønsted acidity of bulk WO_3 has also been calculated in terms of the energy release associated with the formation of pyridine adsorption products. It was found that such process is also exothermic and exergonic with $\Delta H = -93$ and $\Delta G = -45$ kJ mol^{-1}. These values are less negative than those involving dimer IId and monomers Ib and Ie, indicating that the acidity of surface hydroxyl groups in WO_3 is increased when it is supported on zirconia.

A more detailed study has been performed for structure IId, in order to determine whether for dimeric, and larger polymeric WO_x domain, the acidity of all the H in the hydroxylated sites is equivalent. Three different kinds of H sites have been considered (Fig. 5). Those labeled as (A), represent H atoms that would be involved in the condensation process, and that consequently would disappear in the formation of (n + 1)-units polymer from n-units polymeric WO_x. H sites (B) represent those atoms located in non-edge positions of the WO_x domain and that would still be present in the next polymeric unit, while H sites (C) stand for those H atoms that would also remain after condensation but that are involved in intra-molecular interactions, through H bonds formation.

Two local criteria have been analyzed for comparisons among hydrogens A, B and C: atomic charges and condensed Fukui functions (FF). The most positive charge was found on H (A) followed by H (B) and H (C) in that order. The values of the nucleophilic FF also follow the same trend: f_k^+(A) > f_k^+(B) > f_k^+(C). These finding suggest that not all the H in the WO_x domain are equally acid, but that the H atoms at the edge of the domain (A) are the most acid ones, closely followed by H (B), while H (C) are significantly less acid.

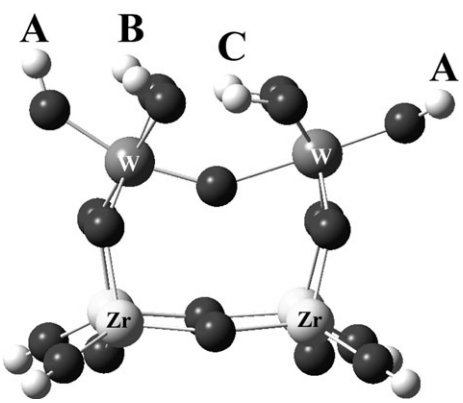

Fig. 5 Different H sites in dimer IId.

Table 3 Charges (q), nucleophilic Fukui functions (f_k^+) for different H sites

	q^a	f_k^+
H (A)	+ 0.192	0.025
H (B)	+ 0.158	0.023
H (C)	+ 0.094	0.013

[a] Hirshfeld partitioning scheme.

These results also suggest that the interactions with pyridine must mainly involve type (A) of H atoms (Table 3).

Additionally, in order to confirm the predictions from the local properties, Gibbs free energies of reaction have been calculated for the interaction of pyridine with the three different H sites (Fig. 5 and 6). The ΔG values, at 298 K were found to be −52.86, −43.35, and −19.08 kJ mol^{-1}, for sites A, B and C, respectively. These values confirm that the acidity of different H sites in dimers, and most likely in higher polymeric units of the WO_x domain, is not the same. They also indicate that the most likely sites for interaction with pyridine are those labeled as A and B, in that order. Our results also suggest that the most acid H disappear due to the condensation process. Accordingly, the formation of polymers with (n + 1) units, from those with n units, not only represent lowering in the number of Brønsted sites, but also a decrease in the acidity per H site. It seems worthwhile to emphasize how relevant a difference in ΔG of 9.5 kJ mol^{-1} (A–B) in terms of relative populations of the corresponding species might be. To make such estimation the following expression was used to estimate the population ratio:

$$\frac{n_A}{n_B} = \exp((\Delta G_{A-B})/RT) \qquad (5)$$

where n_A/n_B is the species A and B population ratio, R is the gas constant and T is the temperature. According to eqn (5), and neglecting the formation of product C, the population of species A and B would be 0.98 and 0.02, respectively, at room temperature.

To gather all of the above discussed results, the values of calculated Brønsted acidity, per H site (A) and in terms of ΔG of reaction with pyridine, and hardness ($\eta^{\text{TD-DFT}}$) for each model have been schematically represented in Fig. 7. For clarity purposes, the structures were arranged following the sequence of calculated hardness values. Each model was represented as a polyhedron making them more familiar with evolution of the system as tungsten loading increases. Two zones can be defined: those where isolated polyhedrons with maximum hardness and maximum acidity predominate and the other one (right) in which mostly dimeric species prevail. Those models corresponding to isolated species (left) should represent the behavior at very low loads of W ($\leq$4 W nm^{-2}) with scarce domains essentially formed by monomeric WO_x. On the other hand, the dimeric models domain simulates better the zone between 4–7 W nm^{-2}, where n-meric domains (mainly dimeric species) of WO_x are expected to be the most abundant ones. The changes in the acidities for tungsten contents $\geq$ 7 W nm^{-2} are explained as a result of the increase in the degree of condensation towards a bulk-like behavior. This implies the loss of most acid sites as well, represented by

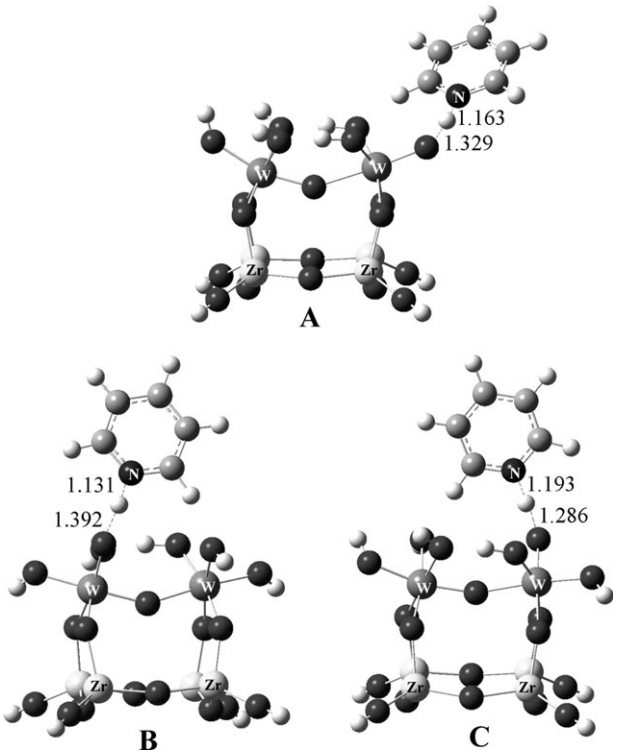

Fig. 6 Fully optimized geometries of the complexes formed by pyridine adsorption on different H sites.

the trends obtained from the calculated models having H site types (A), (B) and (C).

Based on these findings, it seems that for surface densities ≤ 4 W nm^{-2}, mainly monomeric species are present. Brønsted acidity is very low and electronic hardness (η) and Lewis acidity are relatively high. The 5 W nm^{-2} density value represents the transition point where the polymeric/monomeric ratio change. At higher values, presumably the octahedral dimeric species become the most abundant ones, up to 7 W nm^{-2}. The validity of this assignation is consistent with the experimental results reported by Wachs *et al.*[26] According to these authors, the edge energy (E_g) values of bulk tungsten oxide reference compounds with dimeric structure are expected to range from $E_g = 4.3$ ($\eta = 2.15$) to 3.6 ($\eta = 1.8$) eV, in good correspondence with our experimental determination by UV-Vis DRS of $\eta = 2.01$ to $\eta = 1.9$ eV. From this concentration up, species with a higher polymeric degree are expected to prevail. Any WO_x load larger than that is expected to reduce the Brønsted acidity of the WO_x-ZrO_2 system. Thus the theoretical predictions presented in this study provide a viable explanation for the experimental behavior frequently found to a certain value of W surface density in a different catalytic process, particularly in catalyzed reactions which require a maximum of Brønsted acidity.[5,39–42]

Conclusions

The current study demonstrates that the change in acidity, as the W load increases, in WO_x-ZrO_2 systems is a consequence of two main factors: (i) the local coordination and (ii) the polymerization degree of the WO_x domain, which in mutual cooperation produce significant variations on the surface chemical properties.

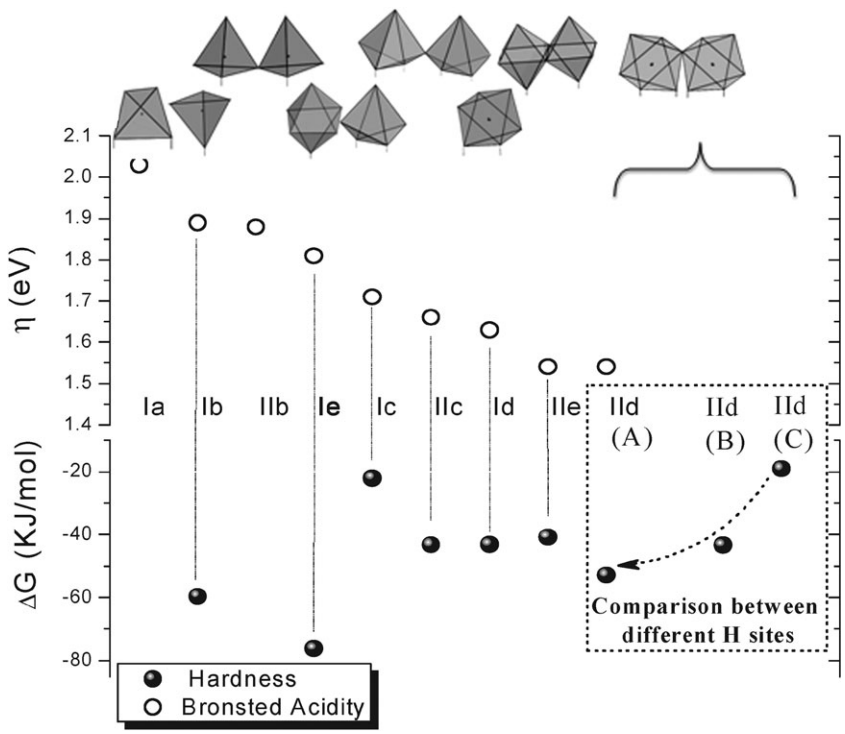

Fig. 7 Schematic representation of the evolution of hardness and Brønsted acidity for each calculated models. The structures were organized following the sequence of the hardness values.

The electronic hardness and Lewis acidity of the WO_x-ZrO_2 systems has been found to decrease with the W loads. This tendency is correctly predicted by the theoretical calculations.

Additionally, it is also predicted that not all the Brønsted sites in the WO_x domain are equally acidic: the sites at the edge of the domain are the most acid ones. Accordingly, as the number of units in the polymeric domains increases the most acid H sites disappear due to the condensation process. This not only represents lowering in the number of Brønsted sites, but also a decrease on the acidity per H site.

The 5 W nm^{-2} value represents the point where the monomeric to polymeric conversion is maximum. At values between 4 and 7 W nm^{-2}, dimeric species are expected to be the most abundant ones, while species with polymeric degree >2 are expected to prevail at concentrations >7 W nm^{-2}. The theoretical quantum calculations predict a maximum Brønsted acidity for octahedral dimeric domains.

References

1. M. Hino and K. Arata, *J. Chem. Soc., Chem. Commun*., 1988, 1259.
2. K. Arata, *Adv. Catal*., 1990, **37**, 165.
3. R. A. Boyse and E. I. Ko, *J. Catal*., 1997, **171**, 191.
4. R. D. Wilson, D. G. Barton, C. D. Baertsch and E. Iglesia, *J. Catal*., 2000, **194**, 175.
5. C. D. Baertsch, K. T. Komala, T.-W. Chua and E. Iglesia, *J. Catal*., 2002, **205**, 44.
6. S. Lecarpentier, J. van Gestel, K. Thomas and M. Houalla, *J. Catal*., 2007, **245**, 45.
7. S. Triwahyono, T. Yamada and H. Hattori, *Appl. Catal., A*, 2003, **242**, 101.
8. S. De Rossi, G. Ferraris, M. Valigi and D. Gazzoli, *Appl. Catal., A*, 2002, **231**, 173.
9. P. Afanasiev, C. Geantet, M. Breysse, G. Coudurier, J. C. Vedrine and J. Chem, *J. Chem. Soc., Faraday Trans*., 1994, **90**, 193.
10. D. G. Barton, M. Shtein, R. D. Wilson, S. L. Soled and E. Iglesia, *J. Phys. Chem. B*, 1999, **103**, 630.
11. M. A. Cortés-Jacome, C. Angeles-Chavez, E. Lopez-Salina, J. Navarrete, P. Toribio and J. A. Toledo, *Appl. Catal., A*, 2007, **318**, 178.
12. F. D. Gregorio and V. Keller, *J. Catal*., 2004, **225**, 45.
13. A. Iribarren, G. Rodriguez-Gattorno, J. A. Ascencio, A. Medina and E. Torres-Garcia, *Chem. Mater*., 2006, **18**, 5446.
14. E. Torres-García, G. Rosas, J. A. Ascencio, E. Haro-Poniatowski and R. Perez, *Appl. Phys. A*, 2004, **79**, 401.
15. M. J. Frisch, G. W. Trucks, H. B. Schlegel, G. E. Scuseria, M. A. Robb, J. R. Cheeseman, V. G. Zakrzewski, J. A. Montgomery, Jr, R. E. Stratmann, J. C. Burant, S. Dapprich, J. M. Millam, A. D. Daniels, K. N. Kudin, M. C. Strain, O. Farkas, J. Tomasi, V. Barone, M. Cossi, R. Cammi, B. Mennucci, C. Pomelli, C. Adamo, S. Clifford, J. Ochterski, G. A. Petersson, P. Y. Ayala, Q. Cui, K. Morokuma, D. K. Malick, A. D. Rabuck, K. Raghavachari, J. B. Foresman, J. Cioslowski, J. V. Ortiz, B. B. Stefanov, G. Liu, A. Liashenko, P. Piskorz, I. Komaromi, R. Gomperts, R. L. Martin, D. J. Fox, T. Keith, M. A. Al-Laham, C. Y. Peng, A. Nanayakkara, C. Gonzalez, M. Challacombe, P. M. W. Gill, B. Johnson, W. Chen, M. W. Wong, J. L. Andres, C. Gonzalez, M. Head-Gordon, E. S. Replogle and J. A. Pople, *GAUSSIAN 98 (Revision A.3)*, Gaussian Inc, Pittsburgh PA, 1998.
16. J. P. Perdew, K. Burke and Y. Wang, *Phys. Rev. B: Condens. Matter Mater. Phys*., 1996, **54**, 16533 and references therein.
17. T. H. Dunning, Jr and P. J. Hay, *Modern Theoretical Chemistry*, ed. H. F. Schaefer III, Plenum, New York, 1976, vol. 3.
18. (*a*) L. v. Szentpaly, P. Fuentealba, H. Preuss and H. Stoll, *Chem. Phys. Lett*., 1982, **93**, 555; (*b*) H. Stoll, P. Fuentealba, P. Schwerdtfeger, J. Flad, L. V. Szentpaly and H. Preuss, *J. Chem. Phys*., 1984, **81**, 2732; (*c*) P. Fuentealba, H. Preuss, H. Stoll and L. V. Szentpaly, *Chem. Phys. Lett*., 1989, **89**, 418.
19. R. G. Parr and R. G. Pearson, *J. Am. Chem. Soc*., 1983, **105**, 7512.
20. E. Runge and E. K. U. Gross, *Phys. Rev. Lett*., 1984, **52**, 997.
21. (*a*) D. Sundholm, *Chem. Phys. Lett*., 1999, **302**, 480; (*b*) A. Dreuw, B. D. Dunietz and M. Head-Gordon, *J. Am. Chem. Soc*., 2002, **124**, 12070; (*c*) A. Tsolakidis and E. Kaxiras, *J. Phys. Chem. A*, 2005, **109**, 2373.
22. (*a*) A. Dreuw and M. Head-Gordon, *J. Am. Chem. Soc*., 2004, **126**, 4007; (*b*) A. Dreuw and M. Head-Gordon, *Chem. Rev*., 2005, **105**, 4009.
23. B. Delley, *J. Chem. Phys*., 1990, **92**, 508.
24. B. Delley, *J. Chem. Phys*., 2000, **113**, 7756.
25. F. L. Hirshfeld, *Theor. Chim. Acta*, 1977, **44**, 129.
26. I. E. Ross-medgaarden and E. I. Wachs, *J. Phys. Chem. C*, 2007, **111**, 15089.
27. M. Valigi, D. Gazzoli, I. Pettiti, G. Matti, S. Colonna, S. De Rossi and G. Ferraris, *Appl. Catal., A*, 2002, **231**, 159.
28. C. Angeles-Chavez, M. A. Cortes-Jacome, E. Torres-García and J. A. Toledo-Antonio, *J. Mater. Res*., 2006, **21**, 807.
29. A. Satsuma, H. Yokoi, H. Nishiyama, S. Kakimoto, S. Sugaya, T. Oshima and T. Hattori, *Chem. Lett*., 2004, **33**, 1250.
30. C. Lahousse, A. Aboulyt, F. Maugé, J. Bachelier and J. C. Lavally, *J. Mol. Catal*., 1993, **84**, 283.
31. E. P. Parry, *J. Catal*., 1963, **2**, 371.
32. C. E. Emeis, *J. Catal*., 1963, **141**, 347.
33. T. Kim, A. Burrow, J. C. Kiely and E. I. Wachs, *J. Catal*., 2007, **246**, 370.
34. Q. Sun, B. K. Rao, P. Jena, D. Stolcic, Y. D. Kim, G. Gantefor, Jr and A. W. Castleman, *J. Chem. Phys*., 2004, **121**, 9417.
35. E. Broclawik, A. Góra, P. Liguzinski, P. Petelenz and H. A. Witek, *J. Chem. Phys*., 2006, **124**, 054709.
36. R. Z. Khaliullin and A. T. Bell, *J. Phys. Chem. B*, 2002, **106**, 7832.
37. D. J. Rosenberg, B. Bachiller-Baeza, T. J. Dines and J. A. Anderson, *J. Phys. Chem. B*, 2003, **107**, 6526.
38. J. Xu, A. Zheng, J. Yang, Y. Su, J. Wang, D. Zeng, M. Zhang, C. Ye and F. Deng, *J. Phys. Chem. B*, 2006, **110**, 10662.
39. M. A. Cortés-Jácome, J. A. Toledo, C. Angeles-Chavez, M. Aguilar and J. A. Wang, *J. Phys. Chem. B*, 2005, **109**, 22730.
40. D. G. Barton, M. Shtein, R. D. Wilson, S. L. Soled and E. Iglesia, *J. Phys. Chem. B*, 1999, **103**, 630.
41. Wen-dong Sun, Zhen-bo Zhao, C. Guo, Xing-kai Ye and Y. Wu, *Ind. Eng. Chem. Res*., 2000, **39**, 3717.
42. C. D. Baertsch, S. L. Soled and E. Iglesia, *J. Phys. Chem. B*, 2001, **105**, 1320.

